Differential dynamics of HIV infection in humanized MISTRG versus MITRG mice

Ivic, Sandra ; Rochat, Mary-Aude ; Li, Duo ; Audigé, Annette ; Schlaepfer, Erika ; Münz, Christian ; Manz, Markus G ; Speck, Roberto F

Abstract: Humanized mice are a powerful tool to study HIV in vivo. The recently generated mouse strains MITRG and MISTRG, which differ in human SIRP expression, support an improved human myeloid lineage development from human hematopoietic stem and progenitor cells. The rationale of the study was the characterization of the two mouse strains during an HIV infection with CCR5- and CXCR4-tropic viruses. Upon HIV infection, we observed HIV dissemination and sustained viral load over 20 wk in peripheral blood in both reconstituted mouse strains. However, HIV RNA levels were significantly lower in MITRG mice compared with MISTRG mice during the first 8 wk postinfection. HIV-infected MISTRG mice showed lymphocyte activation and changes in lymphocyte subsets in blood and spleen, recapitulating hallmarks of HIV infection in humans. Depletion of murine tissue-resident macrophages in MITRG mice led to significantly elevated viral loads, and lymphocyte levels were similar to those in HIV-infected MISTRG mice. Depletion of CD8+ T cells in MISTRG mice before HIV infection resulted in substantially decreased CD4+ T cell levels, indicating functionality of human CD8+ T cells; depletion of CD4+CD8+ thymocytes may have contributed, in part, to the latter finding. In summary, MITRG and MISTRG mice represent novel HIV mouse models, despite differential HIV dynamics.

DOI: https://doi.org/10.4049/immunohorizons.1700042

Differential Dynamics of HIV Infection in Humanized MISTRG versus MITRG Mice

Sandra Ivic, Mary-Aude Rochat, Duo Li, Annette Audigé, Erika Schlaepfer, Christian Münz, Markus G. Manz and Roberto F. Speck

ImmunoHorizons 2017, 1 (8) 162-175
doi: https://doi.org/10.4049/immunohorizons.1700042
http://www.immunohorizons.org/content/1/8/162

ImmunoHorizons is an open access journal published by
The American Association of Immunologists, Inc.,
1451 Rockville Pike, Suite 650, Rockville, MD 20852

ISSN 2573-7732.

ImmunoHorizons

RESEARCH ARTICLE

Infectious Disease

Differential Dynamics of HIV Infection in Humanized MISTRG versus MITRG Mice

Sandra Ivic,*[,1] Mary-Aude Rochat,*[,1] Duo Li,* Annette Audigé,* Erika Schlaepfer,* Christian Münz,[†] Markus G. Manz,[‡] and Roberto F. Speck*

*Department of Infectious Diseases and Hospital Epidemiology, University Hospital Zurich, University of Zurich, 8091 Zurich, Switzerland; [†]Viral Immunobiology, Institute of Experimental Immunology, University of Zurich, 8057 Zurich, Switzerland; and [‡]Department of Hematology, University Hospital Zurich, University of Zurich, 8091 Zurich, Switzerland

ABSTRACT

Humanized mice are a powerful tool to study HIV in vivo. The recently generated mouse strains MITRG and MISTRG, which differ in human SIRPα expression, support an improved human myeloid lineage development from human hematopoietic stem and progenitor cells. The rationale of the study was the characterization of the two mouse strains during an HIV infection with CCR5- and CXCR4-tropic viruses. Upon HIV infection, we observed HIV dissemination and sustained viral load over 20 wk in peripheral blood in both reconstituted mouse strains. However, HIV RNA levels were significantly lower in MITRG mice compared with MISTRG mice during the first 8 wk postinfection. HIV-infected MISTRG mice showed lymphocyte activation and changes in lymphocyte subsets in blood and spleen, recapitulating hallmarks of HIV infection in humans. Depletion of murine tissue-resident macrophages in MITRG mice led to significantly elevated viral loads, and lymphocyte levels were similar to those in HIV-infected MISTRG mice. Depletion of $CD8^+$ T cells in MISTRG mice before HIV infection resulted in substantially decreased $CD4^+$ T cell levels, indicating functionality of human $CD8^+$ T cells; depletion of $CD4^+CD8^+$ thymocytes may have contributed, in part, to the latter finding. In summary, MITRG and MISTRG mice represent novel HIV mouse models, despite differential HIV dynamics. *ImmunoHorizons*, 2017, 1: 162–175.

INTRODUCTION

Humanized mice (hu mice) have become a valuable tool for studying human hematopoiesis in health and disease (1). In the last two decades, different knockouts (i.e., $Rag1/2^{-/-}$ and $Pkrdc^{-/-}$) have made mice more receptive to accepting human xenografts. NOD-SCID$\gamma c^{-/-}$ (NSG), NOD-SCID truncated γc (NOG), NOD $Rag1^{-/-}\gamma c^{-/-}$ (NRG), and $Rag2^{-/-}\gamma c^{-/-}$ mice are the most commonly used mouse strains for humanization (2–4). In the mid-2000s, transplantation of umbilical cord blood–derived $CD34^+$ hematopoietic stem and progenitor cells (HSPCs) into irradiated newborn pups by intrahepatic (4) or i.v. injection (5) was tested and resulted in higher levels of multilineage hematopoiesis than the transplantation of human $CD34^+$ cells into adult mice (6).

Received for publication August 24, 2017. Accepted for publication September 26, 2017.

Address correspondence and reprint requests to: Prof. Roberto F. Speck, University Hospital of Zurich, Raemistrasse 100, 8091 Zurich, Switzerland. E-mail address: roberto.speck@usz.ch

ORCIDs: 0000-0003-2238-2217 (S.I.); 0000-0003-3414-1330 (M.-A.R.); 0000-0002-8453-1137 (R.F.S.).

[1]S.I. and M.-A.R. contributed equally to this work.

S.I. analyzed data and wrote the manuscript; S.I. and M.-A.R. designed and performed experiments; D.L. performed experiments; A.A. coordinated the work with the mice and transplantation of newborn mice; E.S. helped with processing of organs; C.M. and M.G.M. provided conceptual input; M.G.M. provided the mice; and R.F.S. supervised the work and revised the manuscript.

This work was supported by the Swiss National Science Foundation (Grant 31003A_153248/1) and the Human Hemato-Lymphatic Diseases Clinical Research Focus Program of the University of Zurich (to R.F.S.).

Abbreviations used in this article: CLD, clodronate liposome; $hCD45^+$, human $CD45^+$; HSPC, hematopoietic stem and progenitor cell; hu mice, humanized mice; NOG, NOD-SCID truncated γc; NRG, NOD $Rag1^{-/-}\gamma c^{-/-}$; NSG, NOD-SCID$\gamma c^{-/-}$; p.i., postinfection; $TCID_{50}$, 50% tissue culture infectious dose; T_{CM}, central memory T cell; T_{EM}, effector memory T cell; T_{EMRA}, terminally differentiated effector memory T cell; T_N, naive T cell.

The online version of this article contains supplemental material.

https://doi.org/10.4049/immunohorizons.1700042

ImmunoHorizons is published by The American Association of Immunologists, Inc.

Notably, NRG and NSG mice support better engraftment than *Rag2*$^{-/-}\gamma c^{-/-}$ mice (6, 7). The rather modest engraftment in *Rag2*$^{-/-}\gamma c^{-/-}$ mice is explained by the inadequate "don't-eat-me" signal that human cells transmit to murine macrophages. This signal relies on the proper interaction of the ubiquitously expressed human CD47 and SIRPα on myeloid-monocytic cells. Indeed, mice on a NOD background have a SIRPα allele that efficiently recognizes human CD47 and, thus, provides the murine macrophages with the corresponding inhibitory signal (8).

To improve xenograft acceptance in hu mice with a missing CD47–SIRPα interaction, transgenic expression of human SIRPα (9), murine CD47 expression on human cells by lentiviral-mediated gene transfer (10), or more recently, knockout of murine CD47 (11) have been reported. In fact, the SIRPα–CD47 axis leads to decreased engraftment of human acute leukemia stem cells in hu mice on the NOD background (12).

The supply of human cytokines is critical for engraftment and subsequent multilineage hematopoiesis in hu mice. Several human and mouse cytokines were reported to support immune cell homeostasis in both species (13, 14), but human cells remain poorly reactive to some murine cytokines as a result of their low homology (15). Historically, the injection of various cytokines (e.g., IL-3, SCF, GM-CSF) was used to boost human cell engraftment (16–18). In addition, injection of cytokines was reported to enhance the engraftment of distinct populations, such as NK cells, T cells, and plasmacytoid dendritic cells (19–22). To overcome the need for human cytokine administration, which, in general, does not provide physiological levels, human cytokine knock-in strains of immunodeficient mice were engineered. Thus, various knock-in mice of the *Rag2*$^{-/-}\gamma c^{-/-}$ strain were created, bearing human TPO (14), GM-CSF/IL-3 (23), and M-CSF (14).

Two novel humanized mouse models were recently reported (24) that combine the knock-in transgenes of a number of human cytokines (i.e., human M-CSF, IL-3, TPO, and GM-CSF) in *Rag2*$^{-/-}\gamma c^{-/-}$ mice on a mixed Balb/c × 129 background. The mouse strain was named MITRG. The second one, MISTRG, also expresses the human SIRPα through a bacterial artificial chromosome (9). MITRG and MISTRG mice support better human myeloid cell engraftment than the current gold standard NSG mice and closely mirror the human hematopoietic profile (24). In addition to the efficient engraftment of cord blood–derived CD34$^+$, MISTRG mice show superior engraftment of mobilized peripheral blood CD34$^+$ cells and myeloid lineage development in comparison with other mouse strains (25).

HIV is a human-specific virus. Hu mice fill the long-needed gap for conducting in vivo HIV research. Most HIV studies in hu mice were done with humanized *Rag2*$^{-/-}\gamma c^{-/-}$ (26, 27), NOG (28), or NSG (29) mice. Hu mice have been used to study HIV pathogenesis (30–32) and to explore novel therapeutic modalities (33, 34), including gene engineering of an HIV-resistant immune system (35, 36). Naturally, HIV research benefits from the ongoing efforts to improve humanization in mice. Thus, the aim of this study was to explore the value of MITRG and MISTRG mice for studying HIV.

The innate immune system plays an important role during HIV infection. With the development of MITRG and MISTRG mice, we now have the opportunity to study these interactions in a small animal model with a relatively prominent myeloid system. Specifically, we aimed to characterize some aspects of acute and asymptomatic HIV infection, to monitor the differential dynamics of diverse cell types, and to explore whether the absence of human SIRPα would influence viral replication in humanized MITRG mice.

MATERIALS AND METHODS

Generation of hu mice

Humanized MISTRG and MITRG mice were generated essentially as described (24). In brief, newborn MISTRG and MITRG mice were injected intrahepatically with 2.0×10^5 CD34$^+$ HSPCs derived from umbilical cord blood within the first 3 d after birth.

MISTRG and MITRG mice were bred and maintained in individual ventilated cages and were fed autoclaved food and water. Mice were monitored weekly for symptoms or signs of adverse events, according to a standard score sheet. Engraftment was checked in peripheral blood at 9–10 wk of age, and animals with an engraftment > 5% human CD45$^+$ (hCD45$^+$) cells in peripheral blood were used for experiments.

Virus production and infection

Viral stocks were obtained by polyethylenimine-mediated transfection (Polysciences) of HEK293T cells (American Type Culture Collection, Manassas, VA) with p–YU-2 or p–NL4-3 (provided through the National Institutes of Health AIDS Research and Reference Reagent Program). At 48 h after transfection, virus was harvested, filtered (0.22 μm), and frozen at −80°C until use. Viral titers were determined as described (37). Briefly, 50% tissue culture infectious dose ($TCID_{50}$) was determined by infecting human CD8$^+$ T cell–depleted PBMCs from three healthy donors that were stimulated by the addition of IL-2, PHA, and anti-CD3 beads (Dynal 11131D; Life Technologies). Mice were infected i.p. with HIV YU-2 or NL4-3 at 200,000 $TCID_{50}$ per mouse. HIV RNA plasma levels were measured by RT-PCR (AmpliPrep/COBAS TaqMan HIV-1 Test; Roche) at different time points postinfection (p.i.).

CD34$^+$ cell isolation from umbilical cord blood

HSPCs were isolated from human cord blood with anti-CD34 immunomagnetic beads (Miltenyi Biotec, Bergisch Gladbach, Germany) with a yield of 0.5 to 4×10^6 HSPCs (purity ≥ 90%). HSPCs and "nontargeted" fractions were stored frozen in liquid nitrogen until use.

Immunophenotypic analysis of blood and organ cells

The following human cell surface markers were used for immunophenotyping of peripheral blood and splenocytes: CD45, CD33, CD3, CD16, CD14, CD19, NKp46, CD4, CD8, HLA-DR, CD38, CD11b, CD68, and CD163 and murine CD45, CD11b, Ly6C, F4/80, and CD68 (all Abs were purchased from BioLegend, BD Biosciences, and Beckman Coulter). Washing and reagent dilutions were done with PBS or with FACS buffer (PBS containing 2% FBS and 0.05% sodium azide). Before acquisition, cells were fixed with 1% paraformaldehyde (Sigma). All acquisitions were performed on a Cyan ADP (Beckman Coulter) flow cytometer.

https://doi.org/10.4049/immunohorizons.1700042

Data were analyzed with FlowJo 10 software (TreeStar, Ashland, OR). Cellular debris and dead cells were excluded by their light-scattering characteristics or with live/dead fixable stain (Zombie NIR; BioLegend).

Mononuclear phagocytic cell and CD8$^+$ T cell depletion

Mice were treated i.p. with clodronate liposomes (CLDs; http://www.clodronateliposomes.org; 1 mg/20 g body weight) at 9 wk of age, followed by HIV YU-2 infection 48 h later. The maintenance dose was 0.5 mg/20 g body weight once weekly during the course of the experiment. CD8$^+$ T cell depletion was accomplished as described (38). Briefly, 50 μg of anti-CD8$^+$ T cell Ab OKT8 (Bio X Cell) was administered i.p. on three consecutive days, followed by HIV YU-2 infection. CD8$^+$ T cell depletion was maintained by repeating the procedure every 2 wk, and the depletion was monitored in the peripheral blood.

Statistical analysis

Statistical analyses were performed using GraphPad Prism 6 (GraphPad). Data were subjected to an unpaired Mann–Whitney *U* test, Kruskal–Wallis test, or Spearman correlation, as indicated in the figure legends. The obtained *p* values were considered significant at $p < 0.05$.

Study approval

All animal experiments as well as procurement of human cord blood were approved by ethical committees of the University of Zurich and the Federal Veterinary Department. All animal experimentation was approved by the cantonal veterinary office Zurich (#93/2014). The experiments were conducted according to local guidelines and the Swiss animal protection law. Human cord blood was collected with informed written consent of the parents.

RESULTS

Engraftment levels of nonirradiated MISTRG and MITRG mice

Hu MISTRG and MITRG mice with an engraftment > 60%, as assessed by peripheral blood staining for the pan-human leukocyte marker CD45, are at risk for developing anemia over a short time period as the result of inefficient formation of human RBCs and concomitant phagocytosis of mouse RBCs by human macrophages (24). Omitting irradiation prior to transplantation of CD34$^+$ human HSPCs resulted in reduced engraftment, but it decreased the incidence of anemia. Because we opted for an extended period of experimentation, we transplanted without preconditioning and obtained blood engraftment of hCD45$^+$ cells of 31.67 ± 2.94% and 16.53 ± 1.94% (mean ± SEM, $p \leq 0.001$) in MISTRG and MITRG mice, respectively, at 9 wk of age (Fig. 1A).

We also observed differences in human lymphoid and myeloid cell populations in the blood of MISTRG and MITRG mice (Fig. 1B). All immune cell populations had significantly higher reconstitution levels in MISTRG mice than in MITRG mice, with the exception of CD19$^+$ B cells. The differences were most pronounced for CD3$^+$ T cells (20.39 ± 2.83% versus 3.68 ± 0.61%, mean ± SEM, $p < 0.0001$) and CD33$^+$ myeloid cells (11.02 ± 1.07% versus 4.40 ± 0.52%, mean ± SEM, $p < 0.0001$).

Sustained HIV YU-2 infection in MISTRG and MITRG mice

We infected mice with the CCR5-tropic HIV-1 strain YU-2. Four weeks p.i., HIV RNA copy numbers in the peripheral blood were $4.22 \times 10^5 \pm 1.03 \times 10^5$ per milliliter in MISTRG mice and $7.97 \times 10^4 \pm 4.65 \times 10^4$ per milliliter in MITRG mice (mean ± SEM, $p < 0.0001$) (Fig. 2A). Intriguingly, MISTRG mice had a viral peak at 8 wk p.i., and MITRG mice showed a progressive increase in HIV copy number toward the levels observed in MISTRG mice at 16 wk p.i. We noticed substantial differences in the percentages of CD3$^+$ T cells between the groups (Fig. 2B). Initially, in MISTRG mice, 18.42 ± 3.17% of total hCD45$^+$ cells were CD3$^+$ T cells, and their frequency progressively increased to 84.10 ± 8.65% in the peripheral blood during the course of infection (Fig. 2B). In contrast, MITRG mice had low levels (2.74 ± 0.55%) at baseline, increasing up to 37.60 ± 9.28% at 20 wk p.i., which remained significantly below the CD3$^+$ T cell frequency in MISTRG mice. Within the CD3$^+$ T cell population, CD4$^+$ T cells in MISTRG mice expanded up to week 8 p.i., when HIV replication peaked, and then

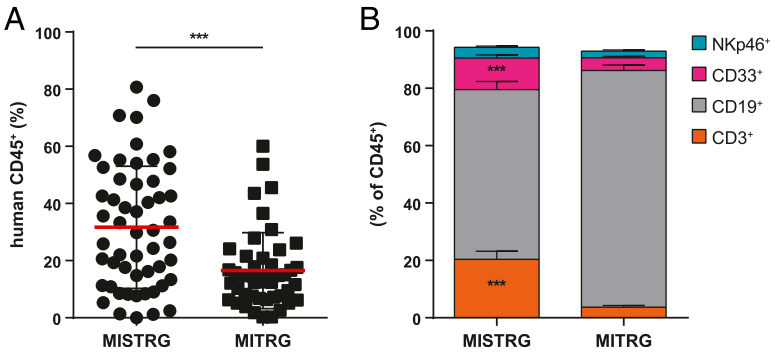

FIGURE 1. Efficient engraftment of nonirradiated MISTRG and MITRG mice at 9 wk of age.

Newborn MISTRG and MITRG mice were transplanted with umbilical cord blood–derived CD34$^+$ HSPCs without irradiation. (**A**) Blood engraftment of 9-wk-old MISTRG (n = 53) and MITRG (n = 47) mice. (**B**) Percentages of different cell populations of lymphoid and myeloid lineages gated on hCD45$^+$ cells. All data are mean ± SEM. ***$p \leq 0.001$, two-tailed Mann–Whitney *U* test.

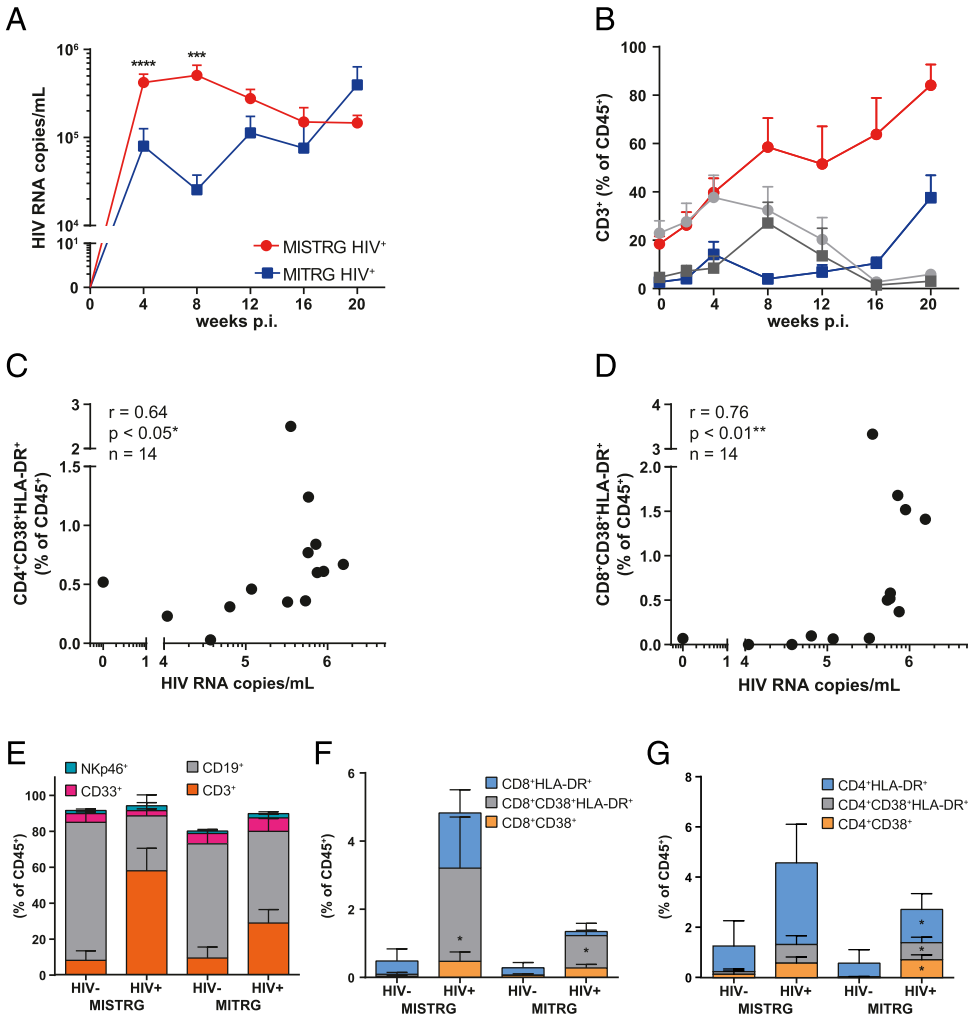

FIGURE 2. Sustained HIV infection with CCR5-tropic YU-2 in MISTRG and MITRG mice.

After confirmation of hCD45$^+$ cell (>5% in blood) engraftment, humanized MISTRG and MITRG mice were infected with HIV-1 YU-2. (**A**) HIV RNA copy numbers were measured in the plasma over time (MISTRG, n = 6–21; MITRG, n = 4–20). (**B**) CD3$^+$ T cell percentages, gated on hCD45$^+$ cells, in peripheral blood shown for MISTRG mice (HIV$^+$ = red circles and HIV$^-$ = gray circles) and MITRG mice (HIV$^+$ = blue squares and HIV$^-$ = gray squares). Spearman correlation between the percentages of CD4$^+$CD38$^+$HLA-DR$^+$ cells (**C**) and CD8$^+$CD38$^+$HLA-DR$^+$ cells (**D**) (of hCD45$^+$ cells) and HIV RNA copies per milliliter in plasma at 4 wk p.i. (**E**) Distribution of different cell populations in spleen at sacrifice for uninfected mice (MISTRG, n = 3; MITRG, n = 9) and infected mice (MISTRG, n = 7; MITRG, n = 6). Frequencies of activated CD8$^+$ T cells (**F**) and CD4$^+$ T cells (**G**) (of hCD45$^+$ cells) in spleen. All data are mean ± SEM. Statistical differences between groups at different times were calculated using the two-tailed Mann–Whitney U test (A and B) and the Kruskal–Wallis test with the Dunn multiple-comparison test (E–G). *$p < 0.05$, **$p \leq 0.01$, ***$p \leq 0.001$, ****$p \leq 0.0001$.

declined (Supplemental Fig. 1). In contrast, levels of CD8$^+$ T cells constantly increased (Supplemental Fig. 1).

HIV infection promotes immune activation of T cells. In MISTRG mice, we observed a positive correlation between the viral load in the plasma and CD38$^+$ HLA-DR$^+$ CD4$^+$ T cells (Fig. 2C) and CD8$^+$ T cells (Fig. 2D) in the blood at week 4 p.i.. These analyses were not conclusive in MITRG mice because of the low CD3$^+$ T cell numbers.

At sacrifice at 12 or 20 wk p.i., we observed similar distributions of cell populations in the spleen (Fig. 2E) as in the blood (Fig. 1B) of uninfected MISTRG and MITRG mice. In infected animals, a substantial increase in the percentage of splenic CD3$^+$ T cells compared with uninfected ones was observed in both strains, particularly in MISTRG mice (8.02 ± 5.28% versus 58.00 ± 12.54% CD3$^+$ T cells of hCD45$^+$ cells, $p = 0.033$). We also noted increases in the activation of CD8$^+$ and CD4$^+$ splenocytes in MISTRG mice, as well as in MITRG mice, as quantified by the expression of CD38 and HLA-DR (Fig. 2F, 2G).

Changes in differentiation subsets of CD4$^+$ and CD8$^+$ T cells in MISTRG mice during acute and chronic HIV infection

HIV infection in humans is divided into three stages: acute HIV infection (the first 12 wk after transmission), chronic HIV infection, and the late stage, known as AIDS. Similarly, in our experiments, we defined acute infection as the first 12 wk p.i.

https://doi.org/10.4049/immunohorizons.1700042

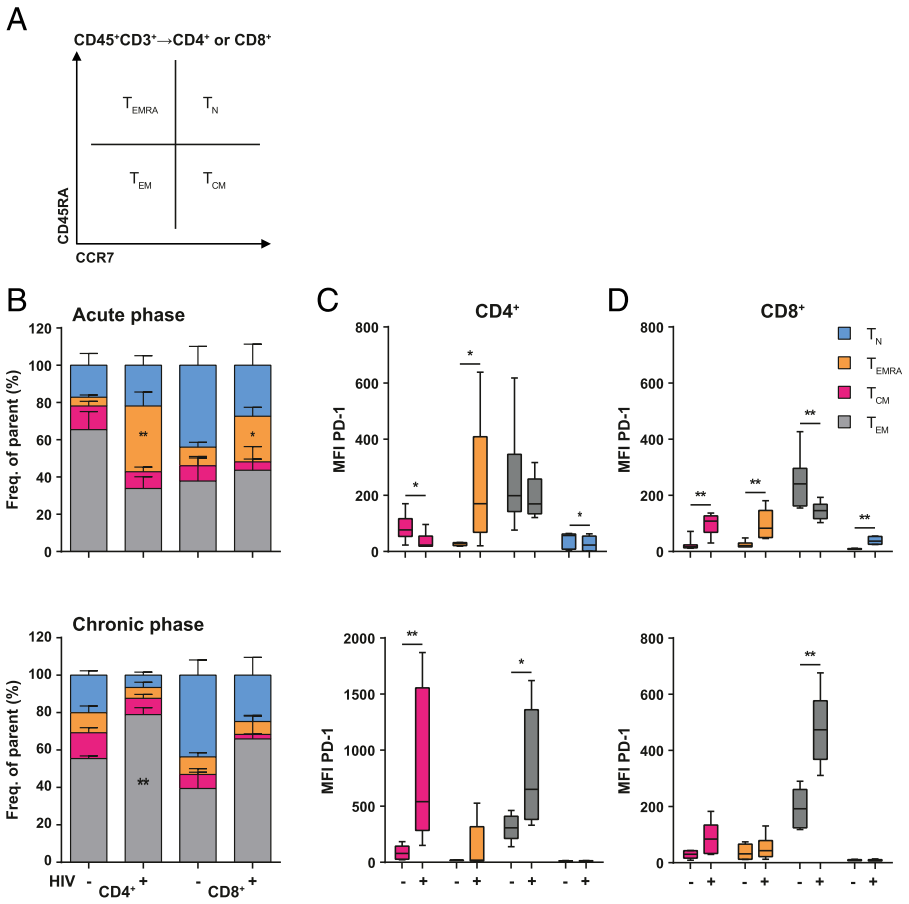

FIGURE 3. Changes in splenic CD4$^+$ and CD8$^+$ T cell subsets during acute and chronic HIV infection in MISTRG mice.

MISTRG mice infected with YU-2 were sacrificed 5 or 12–20 wk p.i., and splenocytes were analyzed for differentiation and PD-1 expression. (**A**) Definition of T cell differentiation subsets. (**B**) Frequency of T_N (blue), T_{EMRA} (orange), T_{CM} (pink), and T_{EM} (gray) in CD4$^+$ and CD8$^+$ T cell subsets in the spleen during acute infection (upper panel) (MISTRG HIV$^-$, n = 7; HIV$^+$, n = 6) and chronic infection (lower panel) (MISTRG HIV$^-$, n = 6, HIV$^+$, n = 6). Median fluorescent intensity of PD-1 in uninfected and infected MISTRG mice on CD4$^+$ (**C**) and CD8$^+$ (**D**) T cell subsets in acute (upper panels) and chronic (lower panels) HIV infection. Data are mean ± SEM. *$p < 0.05$, **$p < 0.01$, two-tailed Mann–Whitney U test.

and chronic infection from 12 wk p.i. on (39). Thus, we sacrificed MISTRG mice at 5 and 12–20 wk p.i. to investigate changes within the T cell compartment in the spleen by flow cytometry and compared them with age-matched uninfected MISTRG mice (Fig. 3A).

Within CD4$^+$ splenocytes, we observed a slight increase in CD45RA$^+$CCR7$^+$ naive T cells (T_N) and CD45RA$^+$CCR7$^-$ terminally differentiated effector memory T cells (T_{EMRA}), whereas CD45RA$^-$CCR7$^-$ effector memory T cells (T_{EM}) and CD45RA$^-$CCR7$^+$ central memory T cells (T_{CM}) showed a tendency to decrease in infected MISTRG mice during acute infection compared with uninfected mice (Fig. 3B). During the chronic phase, we observed a shift from T_{EMRA} to T_{EM} in the CD4$^+$ T cell compartment, with a concomitant decrease in T_N in comparison with uninfected MISTRG mice.

During the acute phase of infection, T_{EM} and T_{CM} remained stable among CD8$^+$ T cells, but there was a significant increase in T_{EMRA} and concomitantly lower frequencies of T_N (Fig. 3B). Similar to the CD4$^+$ T cell compartment, we observed a trend for a shift from T_{EMRA} to T_{EM} among CD8$^+$ T cells ($p = 0.1175$) compared with uninfected animals.

Notably, the expression of PD-1 is upregulated on terminally differentiated T cells after their activation during acute viral infections (40). Thus, we assessed the median fluorescent intensity of PD-1 in CD4$^+$ splenocytes, which revealed a differential expression (Fig. 3C). The expression of PD-1 was significantly elevated in CD4$^+$ T_{EMRA}; however, it was downregulated during the acute phase of infection in all other subsets. In the chronic phase, PD-1 levels on T_{EMRA} remained comparable to those during acute infection, whereas a substantial increase was observed in T_{CM} ($p = 0.0043$) and T_{EM} ($p = 0.026$).

In CD8$^+$ splenocyte subsets, PD-1 expression was increased on T_N, T_{CM}, and T_{EMRA} (Fig. 3D). A significant decrease in PD-1 was detected on T_{EM} during acute infection. In the chronic phase, only PD-1 levels on T_{EM} were significantly increased ($p = 0.0043$) (Fig. 3D).

Overall, this dynamic of cellular changes indicated an ongoing immune response upon HIV infection. However, hCD45$^+$ splenocytes isolated from animals during acute infection and

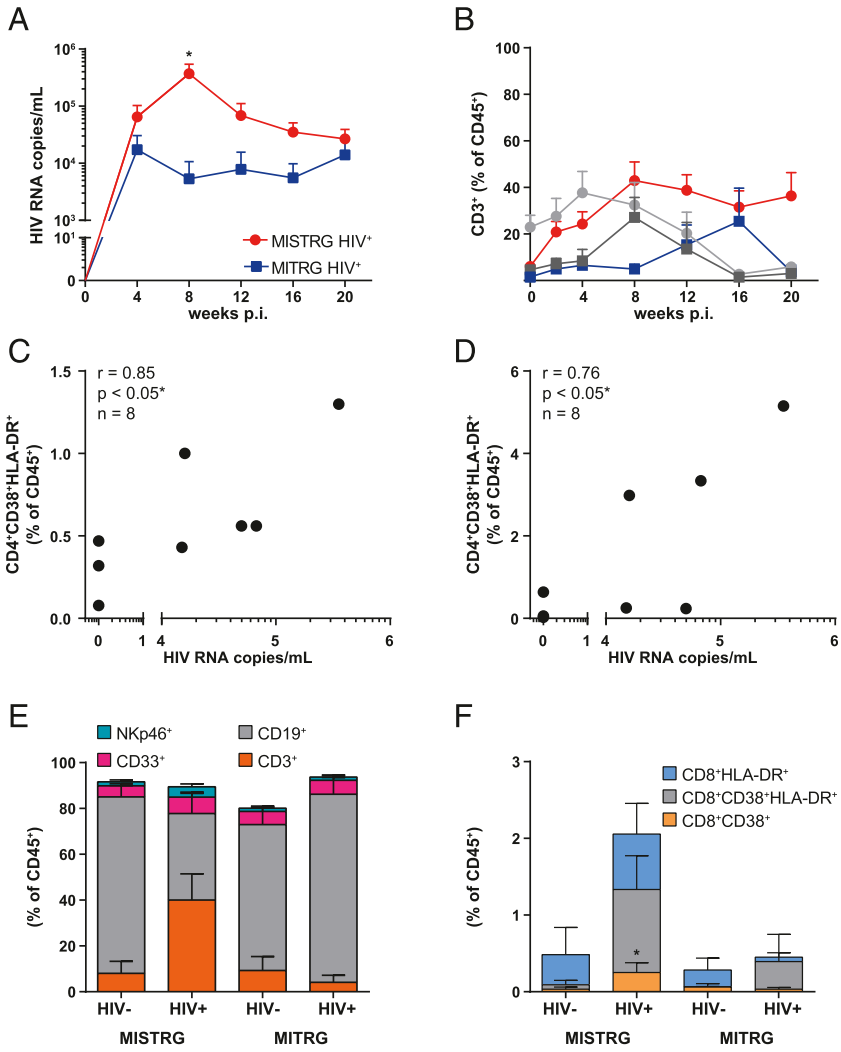

FIGURE 4. Sustained HIV infection with CXCR4-tropic NL4-3 in MISTRG and MITRG mice.

Analogously to YU-2 infection, mice were infected with 200,000 $TCID_{50}$ of NL4-3. (**A**) HIV RNA copy numbers were measured in the plasma in MISTRG mice (HIV^+ = red circles) and MITRG mice (HIV^+ = blue squares). (**B**) Percentages of $CD3^+$ cells in uninfected as well as in HIV-infected MISTRG and MITRG mice (HIV^+ MISTRG mice = red circles; HIV^- MISTRG mice = gray circles; HIV^+ MITRG mice = blue squares; HIV^- MITRG mice = gray squares). (**C** and **D**) Spearman correlation between the percentages of $CD4^+CD38^+HLA\text{-}DR^+$ cells (C) and $CD8^+CD38^+HLA\text{-}DR^+$ cells (D) (of $hCD45^+$ cells) and HIV RNA copies per milliliter in plasma at 4 wk p.i. (**E**) Distribution of different cell types in the spleen at euthanasia for uninfected mice (MISTRG, $n = 3$; MITRG, $n = 9$) and infected mice (MISTRG, $n = 8$; MITRG, $n = 3$) at 12 and 20 wk p.i. (**F**) Frequencies of activated $CD8^+$ T cells of $hCD45^+$ cells in spleen. All data are mean ± SEM. Statistical differences between groups at different times were calculated by the two-tailed Mann–Whitney *U* test (A and B) and the Kruskal–Wallis test with the Dunn multiple-comparison test (E and F). $*p < 0.05$.

stimulated with Env and Gag HIV peptide pools did not demonstrate HIV-specific IFN-γ or TNF-α responses (data not shown).

Sustained HIV NL4-3 infection in MISTRG and MITRG mice

We also infected MISTRG and MITRG mice with the CXCR4-tropic strain, NL4-3. Similar to infection with the CCR5-tropic strain, YU-2, HIV replication was higher in MISTRG mice than in MITRG mice (Fig. 4A). In MISTRG mice, plasma viral loads of $3.30 \times 10^5 \pm 1.56 \times 10^5$ HIV RNA copies per milliliter peaked at 8 wk p.i. and decreased thereafter, whereas in the MITRG group, viremia plateaued at 4 wk p.i. with $5.84 \times 10^4 \pm 3.42 \times 10^4$ copies per milliliter. Remarkably, we could not infect 5 of 12 MITRG mice, despite reasonable engraftment levels of 11.33 ± 1.81% $hCD45^+$ cells in the peripheral blood (data not shown).

The level of $CD3^+$ T cells in the peripheral blood continuously increased until 8 wk p.i. in MISTRG mice infected with NL4-3, despite vigorous HIV replication (Fig. 4B); however, this expansion was lower than in mice infected with YU-2 (Fig. 2B). We also detected increasing levels of $CD3^+$ T cells in MITRG mice at 12 wk p.i with NL4-3, which was at an earlier time point than in

https://doi.org/10.4049/immunohorizons.1700042

MITRG mice infected with YU-2. In both infection models, the $CD4^+$ T cell percentage was lower in infected mice than in the uninfected control groups, displaying the highly cytopathic nature of CXCR4-tropic strains (41) (Supplemental Fig. 1).

In accordance with data generated during CCR5-tropic infection, we detected $CD38^+HLA\text{-}DR^+$ $CD4^+$ (Fig. 4C) and $CD8^+$ (Fig. 4D) T cells at 4 wk p.i., the percentages of which correlated with HIV RNA copy numbers in the plasma.

Similar to YU-2 infection, we found more $CD3^+$ T cells in the spleens of NL4-3–infected MISTRG mice than in uninfected MISTRG mice (Fig. 4E). In contrast, we did not observe any increase in T cells in MITRG mice. Cellular subset analysis revealed more activated $CD38^+$ $HLA\text{-}DR^+$ $CD8^+$ splenocytes in HIV-infected mice than in uninfected ones (Fig. 4F).

No effect of $CD8^+$ T cell depletion on HIV viral load in MISTRG mice

We observed a tendency for decreasing viral loads after 8 wk p.i. in MISTRG mice infected with the CCR5- or CXCR4-tropic strain (Figs. 2A, 4A). We hypothesized that $CD8^+$ T cells were responsible for this observation. We depleted $CD8^+$ T cells by administering the anti-human mAb OKT8 to MISTRG mice before HIV infection. To maintain depletion, we administered OKT8 every 2 wk until the mice were sacrificed 5 wk later. The depletion was efficient because we did not detect any $CD8^+$ T cells in the peripheral blood (Fig. 5A). We did not detect differences in viral load with or without $CD8^+$ T cells in MISTRG mice (Fig. 5B). Notably, we observed a trend of a less steep increase in viral load in $CD8^+$ T cell–depleted animals at 2 wk p.i.; this could be due to an OKT8-mediated depletion of $CD4^+CD8^+$ thymocytes and an overall decrease in $CD3^+$ T cell levels (Supplemental Fig. 2), leading to a loss of HIV target cells or the release of chemokines/cytokines by $CD8^+$ T cells. At the end of the experiment, a significant decrease in $CD4^+$ T cell percentage was detected in the spleens and blood (data not shown) of $CD8^+$ T cell–depleted and infected MISTRG mice compared with uninfected $CD8^+$ T cell–depleted animals (Fig. 5C). This probably reflects the combined $CD4^+$ T cell depletion resulting from the reduction of $CD4^+CD8^+$ thymocytes by the OKT8 Ab and the destruction of $CD4^+$ T cells by HIV.

We administered OKT8 to MITRG mice as well. In contrast to HIV-infected and $CD8^+$ T cell–depleted MISTRG mice, we observed a tendency toward a decreased viral load in OKT8-treated MITRG mice (Supplemental Fig. 3). Similar to OKT8-treated MISTRG mice, this might be linked to the diminished $CD3^+$ T cell levels (Supplemental Fig. 3). In addition, MITRG mice receiving OKT8 showed decreased levels of $CD4^+$ T cells during infection compared with uninfected controls, suggesting

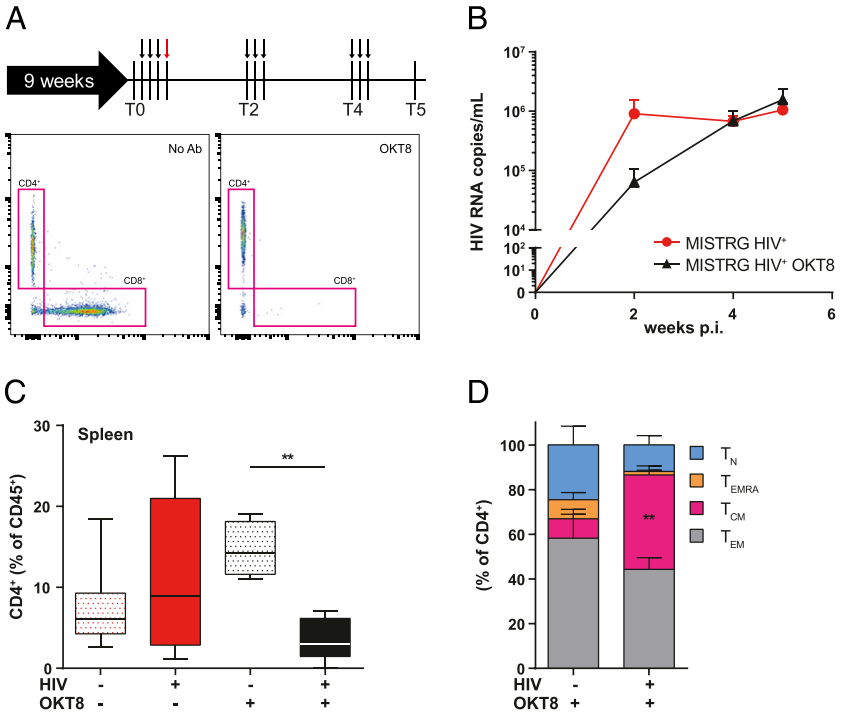

FIGURE 5. Viral load and $CD4^+$ T cells in $CD8^+$ T cell–depleted YU-2–infected MISTRG mice.

(**A**) Depletion protocol: 9-wk-old MISTRG mice were treated on three consecutive days with 50 μg of OKT8 (black arrows), followed by infection with 200,000 $TCID_{50}$ of YU-2 (red arrow). Depletion was confirmed in the peripheral blood by flow cytometry at different times (T0, T2, T4, and T5 wk). (**B**) HIV viral load (MISTRG HIV^+, n = 5–10; MISTRG HIV^+ OKT8, n = 8–10). (**C**) $CD4^+$ T cell frequencies in the spleen after sacrifice at 5 wk p.i. (MISTRG HIV^- [red stippled bar], n = 7; MISTRG HIV^+ [red bar], n = 6; MISTRG HIV^+ OKT8 [black bar], n = 8; MISTRG HIV^- OKT8 [black stippled bar], n = 4). $^{**}p < 0.01$, Kruskal–Wallis test with the Dunn multiple-comparison test. Data are mean ± SEM. (**D**) Distribution of different $CD4^+$ T cell subsets in the spleen at 5 wk p.i. $^{**}p < 0.01$, two-tailed Mann–Whitney U test.

$CD4^+CD8^+$ thymocyte depletion or HIV-mediated $CD4^+$ T cell destruction. In addition, we investigated the distribution of $CD4^+$ splenocyte subsets as depicted (Fig. 3A). $CD8^+$ T cell–depleted uninfected mice showed no significant differences (Fig. 5D) from untreated uninfected controls (Fig. 3B). Upon YU-2 infection in depleted animals, a significant increase in the T_{CM} compartment was detected, with concomitant decreases in T_N, T_{EMRA}, and T_{EM} (Fig. 5D) compared with uninfected OKT8-treated MISTRG mice.

HIV replication profile in MISTRG mice restored in MITRG mice by phagocytic cell depletion

MITRG and MISTRG are identical mouse strains that differ only in the expression of human SIRPα. We hypothesized that the differences in viral load and percentage of $CD3^+$ T cells seen between HIV-infected MITRG and MISTRG mice are caused by expression of human SIRPα on murine cells. To simulate a situation free of phagocytic cells in MITRG mice, and therefore recapitulate some of the features of MISTRG mice, we administered CLDs to MITRG mice. Briefly, MITRG mice were treated with CLDs, followed by YU-2 infection 48 h later (Fig. 6A). The depletion was maintained by repeated weekly injections of CLDs for 3 wk. The CLD protocol used was very efficient, because we did not find any murine $CD68^+F4/80^+$ tissue-resident macrophages in the spleen at euthanasia. The CLD treatment administered for 3 wk led to a higher blood engraftment level than the mock treatment (PBS: 12.67 ± 1.82%, CLD: 30.65 ± 4.86% $hCD45^+$ [mean ± SEM], $p = 0.0221$) (Fig. 6B). The HIV load was three-log higher in CLD-treated mice than in mock-treated mice (Fig. 6C). The eventual viral load of the CLD group was even greater than that in HIV-infected MISTRG mice (Fig. 2A). Remarkably, the depletion of phagocytic cells in MISTRG mice promoted further HIV replication (Supplemental Fig. 4).

CLD treatment also resulted in some remarkable cellular changes in the blood: we observed an increase in $NKp46^+$ cells in HIV-infected MITRG mice (Fig. 6D). Similar to previously observed increases in activated $CD4^+$ and $CD8^+$ T cells in YU-2–infected MISTRG mice, we detected elevated levels in CLD-treated MITRG mice (Fig. 6E). However, we did not detect activated T cells in CLD-treated MISTRG mice (Supplemental Fig. 4).

Human cell engraftment was substantially elevated, up to ~40% of $hCD45^+$ cells, in spleens of CLD-treated MITRG mice (Fig. 6F). Splenic cell distributions resembled those in the peripheral blood of MISTRG mice at 9 wk of age (Fig. 1B). Significantly, more $CD3^+$ splenocytes were observed in uninfected and infected CLD-treated MITRG mice than in PBS control mice. Furthermore, we found a significant increase in human $CD68^+CD163^-$ and $CD68^+CD163^+$ splenic macrophages in CLD-treated mice, irrespective of HIV infection (PBS $p = 0.008$) (Fig. 6F). Moreover, HIV infection alone appeared to induce expansion of $CD68^+CD163^+$ macrophages.

Taken together, the depletion of macrophages in MITRG mice reproduced, in essence, the data observed in MISTRG mice and supports our hypothesis that the expression of human SIRPα on murine macrophages is at the origin of the differences observed between HIV-infected humanized MITRG and MISTRG mice.

DISCUSSION

In this study, our main findings were that, even without preconditioning, we obtained efficient engraftment levels in MI(S)TRG mice; reconstituted MITRG and MISTRG mice are susceptible to HIV infection with distinct coreceptor selectivity, and the infection is sustained over 20 wk; MITRG mice show a different pattern of HIV infection compared with MISTRG mice, in terms of lower HIV replication and T cell levels; the HIV-replication profile in MISTRG mice is restored in MITRG mice by depleting phagocytic cells, resulting in increased viral loads and higher engraftment levels; and $CD8^+$ T cell depletion in HIV-infected MISTRG mice induces massive $CD4^+$ T cell depletion but has no effect on HIV replication rate. Clodronate treatment removes the negative regulation of xenogenic murine macrophages on human hematopoiesis and allows a faster HIV pathogenesis; thus, the similar HIV-replication pattern in HIV-infected MISTRG mice and macrophage-depleted MITRG mice points to a particular role for SIRPα in these HIV models. Overall, both models are suitable for the study of the interplay between the immune system and HIV.

Irradiation of MISTRG mice promotes liberation of space in the bone marrow niche for injected human $CD34^+$ cells, and high levels of multilineage human hematopoiesis are supported by the knock-in of human cytokines. This, in turn, may result in severe anemia and limited experimentation and lifespan (24). Similar observations were made in $MIS^{(KI)}$TRG mice (42), a novel mouse model similar to MISTRG mice that expresses the human SIRPα from the corresponding mouse locus instead of a bacterial artificial chromosome transgene. Thus, we transplanted newborn mice without any preconditioning with cord blood HSPCs and obtained slightly lower engraftment levels at 9 wk of age than in irradiated animals transplanted with fetal liver–derived HSPCs (24). However, we observed that human peripheral cells waned at ~36 wk of age. Furthermore, MITRG/MISTRG mice also support engraftment with mobilized peripheral blood $CD34^+$ cells from adults (43). Thus, MITRG/MISTRG mice support engraftment of any kind of $CD34^+$ cells, with more prominent engraftment if irradiated prior to transplantation.

Reconstituted MISTRG and MITRG mice showed sustained and robust HIV replication of the CCR5-tropic strain, YU-2, and the CXCR4-tropic strain, NL4-3, over 20 wk (44). This HIV replication was paralleled by an expansion of the $CD3^+$ T cell population in HIV-infected mice; indeed, in the YU-2–infected MISTRG mice, we even observed an initial expansion of $CD4^+$ T cells, followed by a decline, reminiscent of HIV infection in humans. However, we are challenged by the paradoxical waning of human $CD3^+$ T cells over time in uninfected mice. Thus, HIV appears to be a transient stimulus for the human graft. The constellation observed might be due to a less efficient engraftment in mice without preconditioning compared with mice with preconditioning. Notably, reconstitution without preconditioning results in limited lifetime of the human graft (45).

https://doi.org/10.4049/immunohorizons.1700042

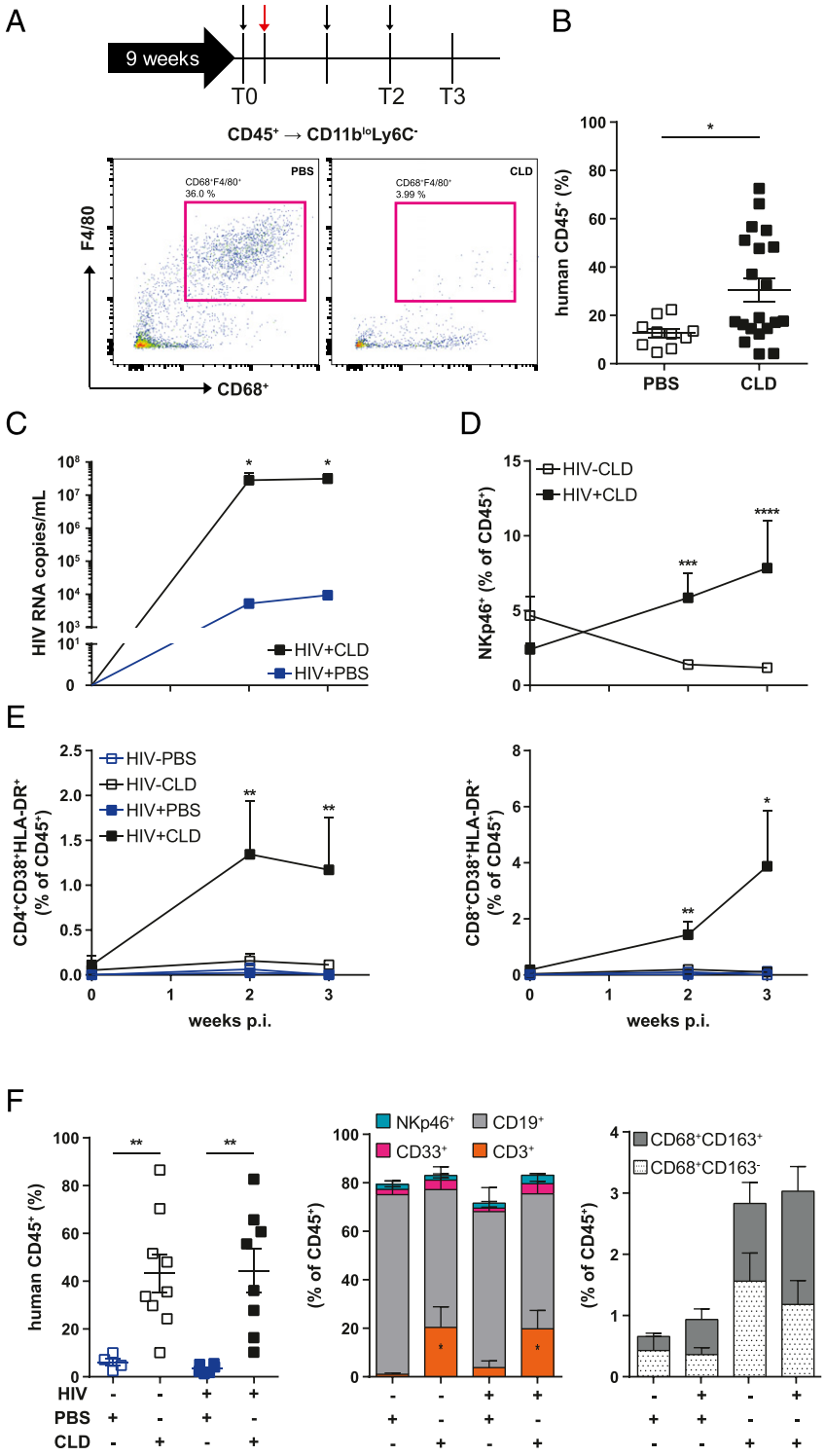

FIGURE 6. Clodronate-mediated mononuclear phagocytic cell depletion induces HIV-replication profile of MISTRG in MITRG mice and elevates viral load levels.

(**A**) Depletion protocol: 9-wk-old MITRG mice were treated with 1 mg of CLDs per 20 g body weight (black arrows), followed by infection with YU-2 (red arrow). Thereafter, the depletion was maintained once weekly, with 0.5 mg per 20 g body weight of CLDs. Depletion was confirmed at the end of the experiment in the spleen by staining for murine tissue-resident macrophages. (**B**) Percentage of hCD45$^+$ cells in the blood at 2 wk p.i.; uninfected mice were pooled with infected mice (PBS, n = 10; CLD, n = 20). (**C**) HIV viral load in CLD-treated (n = 9–11) and PBS-treated (n = 6) MITRG mice. (**D**) NKp46$^+$ cells, as the percentage of hCD45$^+$ cells, in peripheral blood. (**E**) Frequency of activated CD4$^+$ and CD8$^+$ T cells **(Continued)**

We found an increase in $CD4^+$ and $CD8^+$ T_{EMRA} 5 wk p.i., pointing to an immune response against HIV concomitant with a decrease in $CD4^+$ T_{EM}, an HIV target in early infection (46). During the chronic phase, we observed a significant increase in T_{EM} populations. This is most likely explained by a T_{CM} population capable of continuous high-level production of new T_{EM} (46). Comparing the T cell population in the acute versus chronic phases of HIV infection, we observed a prominent contraction of $CD4^+$ T_N, whereas the T_{EM} population expanded, in the chronic phase; the contraction/expansion of $CD4^+$ T cell subsets that we observed was similar to that observed in HIV-infected NSG mice (30). Notably, the distribution of splenic T cell subsets in uninfected MISTRG mice resembled that of reconstituted NSG mice (47) and of healthy humans (48). During acute infection, T_{EMRA} were positive for PD-1 expression, which is a regulator of T cell activation (49) and a marker of exhaustion during viral infections (50, 51). The expression of PD-1 in hu mice was reminiscent of the findings in humans suffering from acute HIV infection (44, 52). However, at the later stage of infection, an increase in PD-1 levels was also observed on $CD4^+$ T_{CM} and T_{EM}, as well as on $CD8^+$ T_{EM}, resembling the findings in individuals in chronic stages of HIV infection

We detected activated $CD4^+$ and $CD8^+$ T cells by means of coexpression of HLA-DR and CD38 in MISTRG mice infected with YU-2. This represents one of the major hallmarks of HIV infection (53–55). The frequencies of activated $CD4^+$ and $CD8^+$ T cells correlated with HIV RNA copy numbers, in line with findings in HIV-infected humans (54). We found lower $CD4^+$ T cell levels during NL4-3 infection, which is explained by the highly cytopathic effect of this virus strain (41, 56). These findings were confirmed by analyzing the cell-activation pattern in the spleen of HIV-infected MISTRG mice, where we found substantially higher frequencies of activated $CD8^+$ splenocytes. Therefore, these two novel humanized mouse models mirror some of the key aspects of acute and chronic HIV infection.

Strikingly, we observed a one-log difference in HIV viral load between MISTRG and MITRG mice, which was apparent at 4–8 wk p.i. and persisted throughout the acute phase. MISTRG mice differ from MITRG mice solely by the transgenic expression of the human don't-eat-me signal, SIRPα. We hypothesized that this signal prevents the clearance of human lymphoid cells, which primarily express CD47, and thereby, promotes the expansion of the pool of potential HIV target cells. It might also prevent the loss of HIV-infected cells. Indeed, MISTRG mice, unlike MITRG mice, showed a progressive increase in $CD3^+$ T cell levels. Thus, we further hypothesized that we can revert this profile by depletion of murine macrophages in MITRG mice. We used CLDs to deplete the mononuclear phagocytic cells and found that CLDs selectively affected the mouse tissue-resident macrophages that develop during embryogenesis (57). In concordance with previous studies (58, 59), the depletion resulted in substantially higher engraftment levels and, indeed, in substantially higher viral loads. Thus, we obtained an HIV-replication profile in MITRG mice resembling MISTRG mice by preventing macrophage-mediated engulfment of human cells with CLDs. In addition to the overall enhanced engraftment levels, depletion of tissue-resident macrophages resulted in elevated levels of $NKp46^+$ cells in the blood at early time points of infection that we did not observe previously in any other experiment. Human $CD68^+CD163^+$ and $CD68^+CD163^-$ macrophages, which most likely have a monocytic origin, were also increased in CLD-treated MITRG mice. We explain the elevated macrophage reconstitution by the overall elevated levels of myeloid cells. We also observed a tendency for increased frequencies of $CD68^+CD163^+$ macrophages in CLD-treated and YU-2–infected animals. Similar observations were reported during SIV infection (60, 61), and soluble CD163 has been suggested as a biomarker for attempts of the immune system to resolve immune activation induced by HIV (62). Thus, data obtained using macrophage-depleted humanized MITRG mice are reminiscent of the data in MISTRG mice and point to a central role for SIRPα expression on macrophages in MISTRG mice for the phenotype observed. The exact role of SIRPα in HIV pathogenesis remains to be determined.

In addition, CLD treatment revealed the same elevation in viral load in MISTRG mice as in MITRG mice, without any increase in engraftment or target cells, excluding an effect related to the proportional amount of target cells. Our observation might be explained by the fact that MISTRG mice express human and murine SIRPα, and a residual phagocytic activity by murine macrophages cannot be excluded. Human macrophages appear to be infected by engulfed HIV-infected $CD4^+$ T cells, which leads to substantially elevated HIV RNA levels in vitro (63).

We also compared the HIV-replication rate of MISTRG/MITRG mice with other humanized mouse models that we used over the years (26, 35, 64, 65). Advantageously, we have been using the identical infection procedure and even the same R5-tropic HIV strain, YU-2. In fact, the extent of HIV replication was the same in MISTRG mice as in hu $Rag2^{-/-}\gamma c^{-/-}$, NOG, and NSG mice; all of these latter hu mice had a distinct overall engraftment level (20.5 ± 22.3, 20.7 ± 13.2, and 48.8 ± 16.7% [average ± SD], respectively, $hCD45^+$ cells of all viable mononucleated cells) that points to factors other than the engraftment level determining the viral-replication rate. The MITRG mice set themselves apart with their one-log lower viral-replication rate, especially in comparison with MISTRG mice.

After the initial viral peak, MISTRG mice exhibited a constant decrease in viral burden and changes in the memory/effector T cell compartments over time. To assess the contribution of $CD8^+$ T cells, we depleted them before HIV infection. Unexpectedly, we did not see any increase in viral load in HIV-infected MISTRG

in blood. (**F**) Percentage of $hCD45^+$ cells (left panel), distribution of different cell types (middle panel), and frequency of macrophage subsets (right panel) in the spleen. Error bars indicate SEM. *$p \leq 0.05$, **$p \leq 0.01$, ***$p \leq 0.001$, ****$p \leq 0.0001$, two-tailed Mann–Whitney *U* test (B–D), Kruskal–Wallis test (E and F).

https://doi.org/10.4049/immunohorizons.1700042

mice, negating a potential $CD8^+$ T cell–driven antiviral effect. These data are in line with a previous study that also found that depletion of $CD8^+$ T cells prior to HIV infection had no effect on lowering HIV (66); in that study, the investigators concluded that acute HIV replication in humanized NSG mice is primarily constrained by the number of available targets in lymphoid tissue rather than by $CD8^+$ T cells. In our hands, however, there were substantially fewer $CD4^+$ T cells in the spleen of depleted and infected animals than in depleted and HIV^- MISTRG mice, and there was a tendency for increased $CD4^+$ T cell levels in infected and undepleted MISTRG mice. This constellation is consistent with a role for $CD8^+$ T cells in preventing $CD4^+$ T cell loss early during HIV infection in $CD34^+$-reconstituted MISTRG mice. Alternatively, we have to consider that the latter finding is strictly due to a depletion of $CD4^+CD8^+$ double-positive thymocytes, with subsequent reduced $CD4^+$ T cell reconstitution. In contrast to the above-discussed findings, HIV-specific $CD8^+$ T cells are present in chronically HIV-infected NSG mice, and their depletion at this later time point resulted in an increase in viral load (67).

In addition, we did not detect any human HIV-specific IgG at 12 and 20 wk p.i., consistent with published data (68). The lack of human HIV-specific IgG is largely explained by the predominance of immature B cells (24). However, some improvement could be achieved by cotransplanting human fetal liver and thymic tissue (69) or the expression of IL-6 (70, 71). These approaches would probably also result in elevated frequencies of HIV-specific T cells. Another limitation was the observation of anemia mainly in MISTRG mice related to high engraftment and leading to their exclusion from experiments, although we did not irradiate them. A solution might be to use fewer HSPCs for transplantation, with possible impairment in engraftment. Notably, we did not observe graft-versus-host disease, which is regularly seen in humanized NSG mice (72), at any time point.

In summary, MITRG and MISTRG mice support HIV replication. Because of superior development of myeloid cells compared with existing humanized mouse models, this model offers the opportunity to study innate immune system modulators (73, 74) and PD-1 inhibitors (75, 76) as treatment for HIV infection. In addition, the roles of CD47 and SIRPα could be studied during infection in MISTRG mice, because the role of this interaction has not yet been defined for HIV, in contrast to cancer and different infectious diseases (77–79). Furthermore, MISTRG mice mirror key features of HIV infection and offer a favorable model to study the various myeloid cell types involved in HIV infection.

DISCLOSURES

The authors have no financial conflicts of interest.

ACKNOWLEDGMENTS

We thank the University Hospital Zurich and Maternité Triemli (Zurich, Switzerland) for cord blood collection. We thank the Department of Immunology, University Hospital Zurich, for the assessment of viral load and HIV-specific Abs. HIV plasmids and peptides were generously provided by the National Institutes of Health AIDS Research and Reference Reagent Program.

REFERENCES

1. Shultz, L. D., M. A. Brehm, J. V. Garcia-Martinez, and D. L. Greiner. 2012. Humanized mice for immune system investigation: progress, promise and challenges. *Nat. Rev. Immunol.* 12: 786–798.
2. Ito, M., H. Hiramatsu, K. Kobayashi, K. Suzue, M. Kawahata, K. Hioki, Y. Ueyama, Y. Koyanagi, K. Sugamura, K. Tsuji, et al. 2002. NOD/SCID/gamma(c)(null) mouse: an excellent recipient mouse model for engraftment of human cells. *Blood* 100: 3175–3182.
3. Shultz, L. D., B. L. Lyons, L. M. Burzenski, B. Gott, X. Chen, S. Chaleff, M. Kotb, S. D. Gillies, M. King, J. Mangada, et al. 2005. Human lymphoid and myeloid cell development in NOD/LtSz-scid IL2R gamma null mice engrafted with mobilized human hemopoietic stem cells. *J. Immunol.* 174: 6477–6489.
4. Traggiai, E., L. Chicha, L. Mazzucchelli, L. Bronz, J. C. Piffaretti, A. Lanzavecchia, and M. G. Manz. 2004. Development of a human adaptive immune system in cord blood cell-transplanted mice. *Science* 304: 104–107.
5. Ishikawa, F., M. Yasukawa, B. Lyons, S. Yoshida, T. Miyamoto, G. Yoshimoto, T. Watanabe, K. Akashi, L. D. Shultz, and M. Harada. 2005. Development of functional human blood and immune systems in NOD/SCID/IL2 receptor gamma chain(null) mice. *Blood* 106: 1565–1573.
6. Brehm, M. A., A. Cuthbert, C. Yang, D. M. Miller, P. DiIorio, J. Laning, L. Burzenski, B. Gott, O. Foreman, A. Kavirayani, et al. 2010. Parameters for establishing humanized mouse models to study human immunity: analysis of human hematopoietic stem cell engraftment in three immunodeficient strains of mice bearing the IL2rgamma(null) mutation. *Clin. Immunol.* 135: 84–98.
7. McDermott, S. P., K. Eppert, E. R. Lechman, M. Doedens, and J. E. Dick. 2010. Comparison of human cord blood engraftment between immunocompromised mouse strains. *Blood* 116: 193–200.
8. Takenaka, K., T. K. Prasolava, J. C. Wang, S. M. Mortin-Toth, S. Khalouei, O. I. Gan, J. E. Dick, and J. S. Danska. 2007. Polymorphism in sirpa modulates engraftment of human hematopoietic stem cells. *Nat. Immunol.* 8: 1313–1323.
9. Strowig, T., A. Rongvaux, C. Rathinam, H. Takizawa, C. Borsotti, W. Philbrick, E. E. Eynon, M. G. Manz, and R. A. Flavell. 2011. Transgenic expression of human signal regulatory protein alpha in $Rag2^{-/-}$ gamma(c)$^{-/-}$ mice improves engraftment of human hematopoietic cells in humanized mice. *Proc. Natl. Acad. Sci. USA* 108: 13218–13223.
10. Legrand, N., N. D. Huntington, M. Nagasawa, A. Q. Bakker, R. Schotte, H. Strick-Marchand, S. J. de Geus, S. M. Pouw, M. Böhne, A. Voordouw, et al. 2011. Functional CD47/signal regulatory protein alpha (SIRP (alpha)) interaction is required for optimal human T- and natural killer- (NK) cell homeostasis in vivo. *Proc. Natl. Acad. Sci. USA* 108: 13224–13229.
11. Lavender, K. J., W. W. Pang, R. J. Messer, A. K. Duley, B. Race, K. Phillips, D. Scott, K. E. Peterson, C. K. Chan, U. Dittmer, et al. 2013. BLT-humanized C57BL/6 Rag2−/−γc−/−CD47−/− mice are resistant to GVHD and develop B- and T-cell immunity to HIV infection. *Blood* 122: 4013–4020.
12. Theocharides, A. P., L. Jin, P. Y. Cheng, T. K. Prasolava, A. V. Malko, J. M. Ho, A. G. Poeppl, N. van Rooijen, M. D. Minden, J. S. Danska, et al. 2012. Disruption of SIRPα signaling in macrophages eliminates human acute myeloid leukemia stem cells in xenografts. *J. Exp. Med.* 209: 1883–1899.
13. Eisenman, J., M. Ahdieh, C. Beers, K. Brasel, M. K. Kennedy, T. Le, T. P. Bonnert, R. J. Paxton, and L. S. Park. 2002. Interleukin-15 interactions with interleukin-15 receptor complexes: characterization and species specificity. *Cytokine* 20: 121–129.

14. Rathinam, C., W. T. Poueymirou, J. Rojas, A. J. Murphy, D. M. Valenzuela, G. D. Yancopoulos, A. Rongvaux, E. E. Eynon, M. G. Manz, and R. A. Flavell. 2011. Efficient differentiation and function of human macrophages in humanized CSF-1 mice. *Blood* 118: 3119–3128.
15. Rongvaux, A., H. Takizawa, T. Strowig, T. Willinger, E. E. Eynon, R. A. Flavell, and M. G. Manz. 2013. Human hemato-lymphoid system mice: current use and future potential for medicine. *Annu. Rev. Immunol.* 31: 635–674.
16. Dao, M. A., K. A. Pepper, and J. A. Nolta. 1997. Long-term cytokine production from engineered primary human stromal cells influences human hematopoiesis in an in vivo xenograft model. *Stem Cells* 15: 443–454.
17. Kamel-Reid, S., and J. E. Dick. 1988. Engraftment of immune-deficient mice with human hematopoietic stem cells. *Science* 242: 1706–1709.
18. Lapidot, T., F. Pflumio, M. Doedens, B. Murdoch, D. E. Williams, and J. E. Dick. 1992. Cytokine stimulation of multilineage hematopoiesis from immature human cells engrafted in SCID mice. *Science* 255: 1137–1141.
19. van Lent, A. U., W. Dontje, M. Nagasawa, R. Siamari, A. Q. Bakker, S. M. Pouw, K. A. Maijoor, K. Weijer, J. J. Cornelissen, B. Blom, et al. 2009. IL-7 enhances thymic human T cell development in "human immune system" Rag2$^{-/-}$IL-2Rgammac$^{-/-}$ mice without affecting peripheral T cell homeostasis. *J. Immunol.* 183: 7645–7655.
20. Kalberer, C. P., U. Siegler, and A. Wodnar-Filipowicz. 2003. Human NK cell development in NOD/SCID mice receiving grafts of cord blood CD34+ cells. *Blood* 102: 127–135.
21. Senpuku, H., T. Asano, K. Matin, M. A. Salam, Y. Tsuha, S. Horibata, Y. Shimazu, Y. Soeno, T. Aoba, T. Sata, et al. 2002. Effects of human interleukin-18 and interleukin-12 treatment on human lymphocyte engraftment in NOD-scid mouse. *Immunology* 107: 232–242.
22. Huntington, N. D., N. Legrand, N. L. Alves, B. Jaron, K. Weijer, A. Plet, E. Corcuff, E. Mortier, Y. Jacques, H. Spits, and J. P. Di Santo. 2009. IL-15 trans-presentation promotes human NK cell development and differentiation in vivo. *J. Exp. Med.* 206: 25–34.
23. Willinger, T., A. Rongvaux, H. Takizawa, G. D. Yancopoulos, D. M. Valenzuela, A. J. Murphy, W. Auerbach, E. E. Eynon, S. Stevens, M. G. Manz, and R. A. Flavell. 2011. Human IL-3/GM-CSF knock-in mice support human alveolar macrophage development and human immune responses in the lung. *Proc. Natl. Acad. Sci. USA* 108: 2390–2395.
24. Rongvaux, A., T. Willinger, J. Martinek, T. Strowig, S. V. Gearty, L. L. Teichmann, Y. Saito, F. Marches, S. Halene, A. K. Palucka, et al. 2014. Development and function of human innate immune cells in a humanized mouse model. *Nat. Biotechnol.* 32: 364–372.
25. Saito, Y., J. M. Ellegast, A. Rafiei, Y. Song, D. Kull, M. Heikenwalder, A. Rongvaux, S. Halene, R. A. Flavell, and M. G. Manz. 2016. Peripheral blood CD34+ cells efficiently engraft human cytokine knock-in mice. *Blood.* 128: 1829–1833.
26. Baenziger, S., R. Tussiwand, E. Schlaepfer, L. Mazzucchelli, M. Heikenwalder, M. O. Kurrer, S. Behnke, J. Frey, A. Oxenius, H. Joller, et al. 2006. Disseminated and sustained HIV infection in CD34+ cord blood cell-transplanted Rag2$^{-/-}$gamma c$^{-/-}$ mice. *Proc. Natl. Acad. Sci. USA* 103: 15951–15956.
27. An, D. S., B. Poon, R. Ho Tsong Fang, K. Weijer, B. Blom, H. Spits, I. S. Chen, and C. H. Uittenbogaart. 2007. Use of a novel chimeric mouse model with a functionally active human immune system to study human immunodeficiency virus type 1 infection. *Clin. Vaccine Immunol.* 14: 391–396.
28. Watanabe, S., K. Terashima, S. Ohta, S. Horibata, M. Yajima, Y. Shiozawa, M. Z. Dewan, Z. Yu, M. Ito, T. Morio, et al. 2007. Hematopoietic stem cell-engrafted NOD/SCID/IL2Rgamma null mice develop human lymphoid systems and induce long-lasting HIV-1 infection with specific humoral immune responses. *Blood* 109: 212–218.
29. Kumar, P., H. S. Ban, S. S. Kim, H. Wu, T. Pearson, D. L. Greiner, A. Laouar, J. Yao, V. Haridas, K. Habiro, et al. 2008. T cell-specific siRNA delivery suppresses HIV-1 infection in humanized mice. *Cell* 134: 577–586.
30. Araínga, M., H. Su, L. Y. Poluektova, S. Gorantla, and H. E. Gendelman. 2016. HIV-1 cellular and tissue replication patterns in infected humanized mice. *Sci. Rep.* 6: 23513.
31. Li, G., M. Cheng, J. Nunoya, L. Cheng, H. Guo, H. Yu, Y. J. Liu, L. Su, and L. Zhang. 2014. Plasmacytoid dendritic cells suppress HIV-1 replication but contribute to HIV-1 induced immunopathogenesis in humanized mice. *PLoS Pathog.* 10: e1004291.
32. Sato, K., T. Izumi, N. Misawa, T. Kobayashi, Y. Yamashita, M. Ohmichi, M. Ito, A. Takaori-Kondo, and Y. Koyanagi. 2010. Remarkable lethal G-to-A mutations in vif-proficient HIV-1 provirus by individual APOBEC3 proteins in humanized mice. *J. Virol.* 84: 9546–9556.
33. Campos, N., R. Myburgh, A. Garcel, A. Vautrin, L. Lapasset, E. S. Nadal, F. Mahuteau-Betzer, R. Najman, P. Fornarelli, K. Tantale, et al. 2015. Long lasting control of viral rebound with a new drug ABX464 targeting Rev-mediated viral RNA biogenesis. *Retrovirology* 12: 30.
34. Horwitz, J. A., A. Halper-Stromberg, H. Mouquet, A. D. Gitlin, A. Tretiakova, T. R. Eisenreich, M. Malbec, S. Gravemann, E. Billerbeck, M. Dorner, et al. 2013. HIV-1 suppression and durable control by combining single broadly neutralizing antibodies and antiretroviral drugs in humanized mice. *Proc. Natl. Acad. Sci. USA* 110: 16538–16543.
35. Myburgh, R., S. Ivic, M. S. Pepper, G. Gers-Huber, D. Li, A. Audigé, M. A. Rochat, V. Jaquet, S. Regenass, M. G. Manz, et al. 2015. Lentivector knockdown of CCR5 in hematopoietic stem and progenitor cells confers functional and persistent HIV-1 resistance in humanized mice. *J. Virol.* 89: 6761–6772.
36. Karpinski, J., I. Hauber, J. Chemnitz, C. Schäfer, M. Paszkowski-Rogacz, D. Chakraborty, N. Beschorner, H. Hofmann-Sieber, U. C. Lange, A. Grundhoff, et al. 2016. Directed evolution of a recombinase that excises the provirus of most HIV-1 primary isolates with high specificity. *Nat. Biotechnol.* 34: 401–409.
37. McDougal, J. S., S. P. Cort, M. S. Kennedy, C. D. Cabridilla, P. M. Feorino, D. P. Francis, D. Hicks, V. S. Kalyanaraman, and L. S. Martin. 1985. Immunoassay for the detection and quantitation of infectious human retrovirus, lymphadenopathy-associated virus (LAV). *J. Immunol. Methods* 76: 171–183.
38. Chijioke, O., A. Müller, R. Feederle, M. H. Barros, C. Krieg, V. Emmel, E. Marcenaro, C. S. Leung, O. Antsiferova, V. Landtwing, et al. 2013. Human natural killer cells prevent infectious mononucleosis features by targeting lytic Epstein-Barr virus infection. [Published erratum appears in 2015 *Cell Rep.* 12: 901.] *Cell Rep.* 5: 1489–1498.
39. Maartens, G., C. Celum, and S. R. Lewin. 2014. HIV infection: epidemiology, pathogenesis, treatment, and prevention. *Lancet* 384: 258–271.
40. Brown, K. E., G. J. Freeman, E. J. Wherry, and A. H. Sharpe. 2010. Role of PD-1 in regulating acute infections. *Curr. Opin. Immunol.* 22: 397–401.
41. Berkowitz, R. D., S. Alexander, C. Bare, V. Linquist-Stepps, M. Bogan, M. E. Moreno, L. Gibson, E. D. Wieder, J. Kosek, C. A. Stoddart, and J. M. McCune. 1998. CCR5- and CXCR4-utilizing strains of human immunodeficiency virus type 1 exhibit differential tropism and pathogenesis in vivo. *J. Virol.* 72: 10108–10117.
42. Deng, K., M. Pertea, A. Rongvaux, L. Wang, C. M. Durand, G. Ghiaur, J. Lai, H. L. McHugh, H. Hao, H. Zhang, et al. 2015. Broad CTL response is required to clear latent HIV-1 due to dominance of escape mutations. *Nature* 517: 381–385.
43. Saito, Y., J. M. Ellegast, A. Rafiei, Y. Song, D. Kull, M. Heikenwalder, A. Rongvaux, S. Halene, R. A. Flavell, and M. G. Manz. 2016. Peripheral blood CD34(+) cells efficiently engraft human cytokine knock-in mice. *Blood* 128: 1829–1833.

44. Breton, G., N. Chomont, H. Takata, R. Fromentin, J. Ahlers, A. Filali-Mouhim, C. Riou, M. R. Boulassel, J. P. Routy, B. Yassine-Diab, and R. P. Sékaly. 2013. Programmed death-1 is a marker for abnormal distribution of naive/memory T cell subsets in HIV-1 infection. *J. Immunol.* 191: 2194–2204.
45. Brehm, M. A., W. J. Racki, J. Leif, L. Burzenski, V. Hosur, A. Wetmore, B. Gott, M. Herlihy, R. Ignotz, R. Dunn, et al. 2012. Engraftment of human HSCs in nonirradiated newborn NOD-scid IL2rγ null mice is enhanced by transgenic expression of membrane-bound human SCF. *Blood* 119: 2778–2788.
46. Okoye, A. A., and L. J. Picker. 2013. CD4(+) T-cell depletion in HIV infection: mechanisms of immunological failure. *Immunol. Rev.* 254: 54–64.
47. Marodon, G., D. Desjardins, L. Mercey, C. Baillou, P. Parent, M. Manuel, C. Caux, B. Bellier, N. Pasqual, and D. Klatzmann. 2009. High diversity of the immune repertoire in humanized NOD.SCID.gamma $c^{-/-}$ mice. *Eur. J. Immunol.* 39: 2136–2145.
48. Sathaliyawala, T., M. Kubota, N. Yudanin, D. Turner, P. Camp, J. J. Thome, K. L. Bickham, H. Lerner, M. Goldstein, M. Sykes, et al. 2013. Distribution and compartmentalization of human circulating and tissue-resident memory T cell subsets. *Immunity* 38: 187–197.
49. Greenwald, R. J., G. J. Freeman, and A. H. Sharpe. 2005. The B7 family revisited. *Annu. Rev. Immunol.* 23: 515–548.
50. Trautmann, L., L. Janbazian, N. Chomont, E. A. Said, S. Gimmig, B. Bessette, M. R. Boulassel, E. Delwart, H. Sepulveda, R. S. Balderas, et al. 2006. Upregulation of PD-1 expression on HIV-specific CD8+ T cells leads to reversible immune dysfunction. *Nat. Med.* 12: 1198–1202.
51. Day, C. L., D. E. Kaufmann, P. Kiepiela, J. A. Brown, E. S. Moodley, S. Reddy, E. W. Mackey, J. D. Miller, A. J. Leslie, C. DePierres, et al. 2006. PD-1 expression on HIV-specific T cells is associated with T-cell exhaustion and disease progression. *Nature* 443: 350–354.
52. Cockerham, L. R., V. Jain, E. Sinclair, D. V. Glidden, W. Hartogenesis, H. Hatano, P. W. Hunt, J. N. Martin, C. D. Pilcher, R. Sekaly, et al. 2014. Programmed death-1 expression on $CD4^+$ and $CD8^+$ T cells in treated and untreated HIV disease. *AIDS* 28: 1749–1758.
53. Giorgi, J. V., and R. Detels. 1989. T-cell subset alterations in HIV-infected homosexual men: NIAID Multicenter AIDS cohort study. *Clin. Immunol. Immunopathol.* 52: 10–18.
54. Deeks, S. G., C. M. Kitchen, L. Liu, H. Guo, R. Gascon, A. B. Narváez, P. Hunt, J. N. Martin, J. O. Kahn, J. Levy, et al. 2004. Immune activation set point during early HIV infection predicts subsequent CD4+ T-cell changes independent of viral load. *Blood* 104: 942–947.
55. Meditz, A. L., M. K. Haas, J. M. Folkvord, K. Melander, R. Young, M. McCarter, S. Mawhinney, T. B. Campbell, Y. Lie, E. Coakley, et al. 2011. HLA-DR+ CD38+ CD4+ T lymphocytes have elevated CCR5 expression and produce the majority of R5-tropic HIV-1 RNA in vivo. *J. Virol.* 85: 10189–10200.
56. Nishimura, Y., C. R. Brown, J. J. Mattapallil, T. Igarashi, A. Buckler-White, B. A. Lafont, V. M. Hirsch, M. Roederer, and M. A. Martin. 2005. Resting naive CD4+ T cells are massively infected and eliminated by X4-tropic simian-human immunodeficiency viruses in macaques. *Proc. Natl. Acad. Sci. USA* 102: 8000–8005.
57. Davies, L. C., and P. R. Taylor. 2015. Tissue-resident macrophages: then and now. *Immunology* 144: 541–548.
58. van Rijn, R. S., E. R. Simonetti, A. Hagenbeek, M. C. Hogenes, R. A. de Weger, M. R. Canninga-van Dijk, K. Weijer, H. Spits, G. Storm, L. van Bloois, et al. 2003. A new xenograft model for graft-versus-host disease by intravenous transfer of human peripheral blood mononuclear cells in $RAG2^{-/-}$ $gammac^{-/-}$ double-mutant mice. *Blood* 102: 2522–2531.
59. Rozemuller, H., S. Knaän-Shanzer, A. Hagenbeek, L. van Bloois, G. Storm, and A. C. Martens. 2004. Enhanced engraftment of human cells in RAG2/gammac double-knockout mice after treatment with CL2MDP liposomes. *Exp. Hematol.* 32: 1118–1125.
60. Tabb, B., D. R. Morcock, C. M. Trubey, O. A. Quiñones, X. P. Hao, J. Smedley, R. Macallister, M. Piatak Jr., L. D. Harris, M. Paiardini, et al. 2013. Reduced inflammation and lymphoid tissue immunopathology in rhesus macaques receiving anti-tumor necrosis factor treatment during primary simian immunodeficiency virus infection. *J. Infect. Dis.* 207: 880–892.
61. Kim, W. K., X. Alvarez, J. Fisher, B. Bronfin, S. Westmoreland, J. McLaurin, and K. Williams. 2006. CD163 identifies perivascular macrophages in normal and viral encephalitic brains and potential precursors to perivascular macrophages in blood. *Am. J. Pathol.* 168: 822–834.
62. Tippett, E., W. J. Cheng, C. Westhorpe, P. U. Cameron, B. J. Brew, S. R. Lewin, A. Jaworowski, and S. M. Crowe. 2011. Differential expression of CD163 on monocyte subsets in healthy and HIV-1 infected individuals. *PLoS One* 6: e19968.
63. Baxter, A. E., R. A. Russell, C. J. Duncan, M. D. Moore, C. B. Willberg, J. L. Pablos, A. Finzi, D. E. Kaufmann, C. Ochsenbauer, J. C. Kappes, et al. 2014. Macrophage infection via selective capture of HIV-1–infected CD4+ T cells. *Cell Host Microbe* 16: 711–721.
64. Nischang, M., R. Sutmuller, G. Gers-Huber, A. Audigé, D. Li, M. A. Rochat, S. Baenziger, U. Hofer, E. Schlaepfer, S. Regenass, et al. 2012. Humanized mice recapitulate key features of HIV-1 infection: a novel concept using long-acting anti-retroviral drugs for treating HIV-1. *PLoS One* 7: e38853.
65. Audigé, A., M. A. Rochat, D. Li, S. Ivic, A. Fahrny, C. K. Muller, G. Gers-Huber, R. Myburgh, S. Bredl, E. Schlaepfer, et al. 2017. Long-term leukocyte reconstitution in NSG mice transplanted with human cord blood hematopoietic stem and progenitor cells. *BMC Immunol.* 18: 28.
66. Petit, N. Y., S. Lambert-Niclot, A. G. Marcelin, S. Garcia, and G. Marodon. 2015. HIV replication is not controlled by CD8+ T cells during the acute phase of the infection in humanized mice. *PLoS One* 10: e0138420.
67. Gorantla, S., E. Makarov, J. Finke-Dwyer, C. L. Gebhart, W. Domm, S. Dewhurst, H. E. Gendelman, and L. Y. Poluektova. 2010. CD8+ cell depletion accelerates HIV-1 immunopathology in humanized mice. *J. Immunol.* 184: 7082–7091.
68. Tanner, A., S. J. Hallam, S. J. Nielsen, G. I. Cuadra, and B. K. Berges. 2015. Development of human B cells and antibodies following human hematopoietic stem cell transplantation to Rag2(−/−)γc(−/−) mice. *Transpl. Immunol.* 32: 144–150.
69. Karpel, M. E., C. L. Boutwell, and T. M. Allen. 2015. BLT humanized mice as a small animal model of HIV infection. *Curr. Opin. Virol.* 13: 75–80.
70. Das, R., T. Strowig, R. Verma, S. Koduru, A. Hafemann, S. Hopf, M. H. Kocoglu, C. Borsotti, L. Zhang, A. Branagan, et al. 2016. Microenvironment-dependent growth of preneoplastic and malignant plasma cells in humanized mice. *Nat. Med.* 22: 1351–1357.
71. Yu, H., C. Borsotti, J. N. Schickel, S. Zhu, T. Strowig, E. E. Eynon, D. Frleta, C. Gurer, A. J. Murphy, G. D. Yancopoulos, et al. 2017. A novel humanized mouse model with significant improvement of class-switched, antigen-specific antibody production. *Blood* 129: 959–969.
72. Sonntag, K., F. Eckert, C. Welker, H. Müller, F. Müller, D. Zips, B. Sipos, R. Klein, G. Blank, T. Feuchtinger, et al. 2015. Chronic graft-versus-host-disease in CD34(+)-humanized NSG mice is associated with human susceptibility HLA haplotypes for autoimmune disease. *J. Autoimmun.* 62: 55–66.
73. Lavender, K. J., K. Gibbert, K. E. Peterson, E. Van Dis, S. Francois, T. Woods, R. J. Messer, A. Gawanbacht, J. A. Müller, J. Münch, et al. 2016. Interferon alpha subtype-specific suppression of HIV-1 infection in vivo. *J. Virol.* 90: 6001–6013.
74. Nian, H., W. Q. Geng, H. L. Cui, M. J. Bao, Z. N. Zhang, M. Zhang, Y. Pan, Q. H. Hu, and H. Shang. 2012. R-848 triggers the expression of TLR7/8 and suppresses HIV replication in monocytes. *BMC Infect. Dis.* 12: 5.

75. Seung, E., T. E. Dudek, T. M. Allen, G. J. Freeman, A. D. Luster, and A. M. Tager. 2013. PD-1 blockade in chronically HIV-1-infected humanized mice suppresses viral loads. *PLoS One* 8: e77780.
76. Porichis, F., and D. E. Kaufmann. 2012. Role of PD-1 in HIV pathogenesis and as target for therapy. *Curr. HIV/AIDS Rep.* 9: 81–90.
77. Willingham, S. B., J. P. Volkmer, A. J. Gentles, D. Sahoo, P. Dalerba, S. S. Mitra, J. Wang, H. Contreras-Trujillo, R. Martin, J. D. Cohen, et al. 2012. The CD47-signal regulatory protein alpha (SIRPa) interaction is a therapeutic target for human solid tumors. *Proc. Natl. Acad. Sci. USA* 109: 6662–6667.
78. Majeti, R., M. P. Chao, A. A. Alizadeh, W. W. Pang, S. Jaiswal, K. D. Gibbs Jr., N. van Rooijen, and I. L. Weissman. 2009. CD47 is an adverse prognostic factor and therapeutic antibody target on human acute myeloid leukemia stem cells. *Cell* 138: 286–299.
79. Li, L. X., S. M. Atif, S. E. Schmiel, S. J. Lee, and S. J. McSorley. 2012. Increased susceptibility to *Salmonella* infection in signal regulatory protein α-deficient mice. *J. Immunol.* 189: 2537–2544.